International Journal of Humanoid Robotics
Vol. 17, No. 5 (2020) 2050015 (20 pages)

DOI: 10.1142/S0219843620500152

Reach to Grasp Planning for a Synergy-Controlled Robotic Hand based on Pesudo-Distance Formulation

Zenghui Liu* and Yuyang Chen†
UM-SJTU Joint Institute, Shanghai Jiao Tong University
800 Dongchuan Rd, Shanghai 200240, P. R. China
**liuzenghui@sjtu.edu.cn*
†supandoria@sjtu.edu.cn

Xiangyang Zhu‡ and Kai Xu§
School of Mechanical Engineering
Shanghai Jiao Tong University
800 Dongchuan Rd, Shanghai 200240, P. R. China
‡mexyzhu@sjtu.edu.cn
§k.xu@sjtu.edu.cn

Received 16 August 2019
Accepted 29 April 2020
Published 21 July 2020

In the past several years, grasp analysis of multi-fingered robotic hands has been actively studied through the use of posture synergies. In these grasping planning algorithms, a formulated optimization is usually performed in the hand's low-dimensional representation together with the hand's position and orientation. The optimization terminates at a stable grasp, often after repeated trials with different initial guesses. Furthermore, there is no guarantee that the generated grasp leads to a smooth reach-to-grasp trajectory since the grasping planning process mostly concerns hand poses with the fingers proximal to the object. A unified theoretical framework of a gradient-based iterative algorithm is hence proposed in this paper to plan a reach-to-grasp task, predicting the grasp quality and adjusting the hand's posture synergies, position and orientation during the approaching phase to achieve a stable grasp. The grasp quality measurement is adopted from a highly efficient pseudo-distance formulation. Stable power grasp and precision pinch can be consistently and intentionally planned with different contact conditions specified in the formulation, which means that an intention for planning a power grasp would not generate a pinch result. Several numerical simulation case studies are presented to demonstrate the effectiveness of the proposed algorithm.

Keywords: Grasp planning; grasp quality; postural synergy; pseudo-distance formulation.

1. Introduction

Humans control multiple muscles in a coordinated manner which is referred to as a postural synergy[1,2] to form a variety of hand postures (e.g., grasps and pinches).

§Corresponding author.

The postural synergies (also called EigenGrasps[3]) have motivated plenty of researches such as mechanical implementations,[4–8] controller realizations,[9–12] grasp planning and analysis,[13–16] resulting from the fact that the postural synergies provide a useful low-dimensional representation of the hand poses.[17] Then the grasp planning problem can be efficiently formulated as an optimization, involving the synergy variables, together with the position and the orientation of the hand.

In the adopted optimization formulations for grasp planning, the optimization often has to be repeated many times with different initial guesses to reach a stable grasp. For example, in the milestone work by Ciocarlie and Allen,[13] a simulated annealing process was used for grasp optimization. The grasp quality is measured as a scaled sum of linear distances and angular alignments between the hand points and the object surface. Several grasping poses during the planning process are shown in Fig. 1(a). It can be seen that the generated intermedium hand poses resulted in a quickly varying (instead of smooth) hand pose trajectories. The simulated annealing algorithm used in a few existing studies[16,18] generated similar results.

In addition, grasp planning as an optimization can also be solved using nonlinear programming, such as (i) the sequential quadratic programming,[15,19] where the objective functions are formulated as the potential energy of the joint springs and the scaled sum of the minimal contact force with a factor concerning defined grasp compatibility, respectively, (ii) the interior-point algorithm,[20] where the objective function is defined as the norm of the finger joint torques, and (iii) the semidefinite programming (SDP),[21] where the objective function is a grasp optimality index that quantifies the force distribution.

In the above grasp planning optimizations, the objective function is usually calculated when the hand is close to the target object. However, a local minimum of the optimization is often reached when the hand is close to the object, which will lead to a

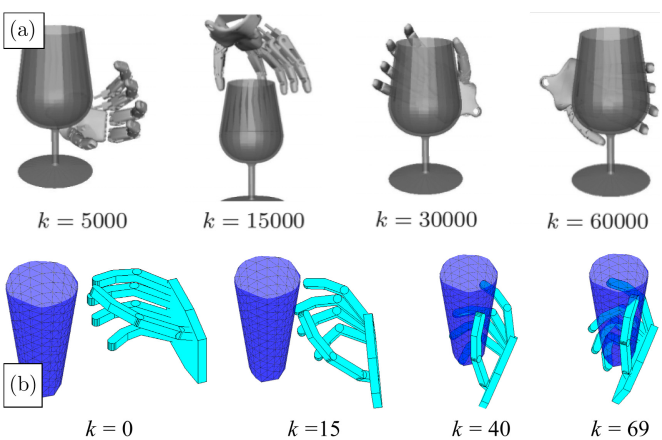

Fig. 1. Reach-to-grasp of anthropomorphic hands: (a) hand poses in Ref. 13 and (b) hand poses using the proposed gradient-based planning.

grasp planning failure. The efficiency of grasp planning is relatively low since a stable grasp is usually achieved after repeated trials. Furthermore, the above grasp planning cannot plan power grasp and precision grasp in a unified way. Due to the deficiency of the available automated grasp planning approaches, synergy-based grasps are also manually planned via the input of a mouse[22] or a myoelectric posture controller.[12]

On the other hand, learning-based grasp planning was also explored. For example, a neural network model based on gradient descent and context fields was trained to generate a grasp configuration output including the pre-grasp and palm orientation, using the visual inputs of an object's location, size, shape, and orientation.[23] Multilayer feed-forward neural networks can be trained to output the hand approaching poses and grasping posture synergies.[24,25] A deep autoencoder network was trained with human data which was acquired from the KIT and YCB object sets to generate the grasp poses.[26] Moreover, the Hidden Markov Model (HMM) can be trained to generate the optimized hand trajectory.[27] However, the generated grasp may not have a guarantee for grasp stability, since the stability is not gauged mathematically during these learning-based processes.

This paper hence presents a gradient-based algorithm for reach-to-grasp planning. The grasp quality is predicted, even when the hand is considerably distant from the object. The position, the orientation, and the postural synergies of the hand are continuously adjusted as the hand approaches the object so that a stable grasp/pinch can be reached with minimal trials. What's more, by including additional points on the finger phalanges and the palm, this proposed framework handles planning of power grasps and precision grasps (a.k.a., pinches) in a unified manner. A few representative poses of a hand reaching and grasping a cup are shown in Fig. 1(b), where the unit of k is the iterations.

A preliminary version of this work was presented at a conference,[28] where only pinch (namely precision grasp) was handled and an sQ distance (scaled Q distance) was defined from the Q distance[29] to predict the grasp quality. In this paper, in order to facilitate the formulation of power grasps where positions of the contact points on the finger phalanges and the palm may change, the pseudo-distance formulation.[30] was introduced here to define a contact Pseudo-distance (cP distance) to quantify the contact condition in the three-dimensional Euclidean space. Then the pseudo-distance formulation is re-written in its particular form in the six-dimensional wrench space, which is equivalent to the Q distance, to measure the grasp quality. In another word, a general form to describe the "distance" between two convex sets in any dimensional space is called pseudo-distance formulation.[30] In this paper, to unify a theoretical framework, the pseudo-distance formulation is written in two forms. One is called cP distance defined in three-dimensional Euclidean space to quantify the contact condition. The other is called Q distance defined in six-dimensional wrench space to quantify the grasp quality.

The differentiability of the pseudo-distance formulation essentially enabled the derivation of the gradient of the status vector which incorporates the cP and the sQ distances. The generalized distance formulation that was proposed in a recent study can also be used except that the derivatives need to be obtained numerically.[31]

Hence, the main contribution of this work lies in the proposal of this unified gradient-based framework for planning reach-to-grasp tasks on a multi-fingered hand for both precision grasps and power grasps. Precision and power grasps can be intentionally planned by specifying different contact conditions on the finger phalanges and/or on the palm. Substantially, more work has been included compared to the preliminary version of this work.[28]

The paper is organized as follows. A derivation summary of the pseudo-distance formulation is reported in Sec. 2, while the description of the synergy-based hand and the formulation of the reach-to-grasp planning algorithm is represented in Sec. 3. Section 4 presents the computational experiments and the conclusion is summarized in Sec. 5.

2. A Summary of the Pseudo-Distance Formulation

The pseudo-distance formulation was originally proposed for the separation and penetration distances between two convex point sets.[30] It can be applied to three-dimensional Euclidian space as well as six-dimensional wrench space. Relevant conclusions are summarized here for readers' convenience.

Given two convex point sets A and B, if they are separated, the separation distance d_s between A and B (a.k.a., the pseudo-distance) is defined as a linear programming problem in Eq. (1).

$$d_s(A,B) = \min \sum_{k=1}^{n_q} \rho_k$$
$$\text{s.t.} \begin{cases} \sum_{k=1}^{n_q} \rho_k \mathbf{q}_k = \sum_{j=1}^{n_b} \beta_j \mathbf{b}_j - \sum_{i=1}^{n_a} \alpha_i \mathbf{a}_i, \quad \rho_k \geq 0, \\ \sum_{i=1}^{n_a} \alpha_i = \sum_{j=1}^{n_b} \beta_j = 1, \quad \alpha_i \geq 0, \quad \beta_j \geq 0 \end{cases} \tag{1}$$

where $\mathbf{q}_k$, $\mathbf{b}_j$, and $\mathbf{a}_i$ are the vertices of the convex sets Q, B, and A; ρ_k, β_j, and α_i are the coefficients for the vertices $\mathbf{q}_k$, $\mathbf{b}_j$, and $\mathbf{a}_i$. n_a, n_b, and n_q are the numbers of the vertices of set A, B, and Q, respectively. To reduce the computational complexity, the set Q is usually selected as a simplex.[30]

When $d_s(A,B)$ gives zero, it means set A intersects with set B or one set envelops the other. Then the penetration distance d_p between A and B is defined as a second linear programming problem in Eq. (2). In this case, value of the pseudo-distance is $d_p(A,\, B)$.

$$d_p(A,B) = \max_{k=1,\ldots,n_q} d_p(k), \tag{2}$$

where $d_p(k)$ for n_q vertices in Q is defined in Eq. (3).

$$d_p(k) = \min(-\rho)$$
$$\text{s.t.} \begin{cases} \rho \mathbf{q}_k = \sum_{i=1}^{n_a} \alpha_i \mathbf{a}_i - \sum_{j=1}^{n_b} \beta_j \mathbf{b}_j, & \rho \geq 0 \\ \sum_{i=1}^{n_a} \alpha_i = \sum_{j=1}^{n_b} \beta_j = 1, & \alpha_i \geq 0, \quad \beta_j \geq 0 \end{cases}, \tag{3}$$

where ρ is a coefficient.

In a particular form of the pseudo-distance formulation that is defined in the six-dimensional wrench space, the pseudo-distance is equivalent to the Q distance.[29] The Q distance formulation for grasp analysis is summarized in the following.

When the hard finger contact model with the Coulomb friction.[32] is used, an object grasped with n contact points is shown in Fig. 2. The friction cone $C(\mathbf{p}_i)$ is linearized by an m-sided polyhedral cone. The cone's edge vectors $\mathbf{d}_1(\mathbf{p}_i), \ldots, \mathbf{d}_m(\mathbf{p}_i)$, satisfying the constraint in Eq. (4):

$$\mathbf{d}_j(\mathbf{p}_i) \cdot \mathbf{n}_i = 1, \quad i = 1, 2, \ldots, n \text{ and } j = 1, 2, \ldots, m, \tag{4}$$

where $\mathbf{n}_i$ is a unit normal vector of the surface at the contact point $\mathbf{p}_i$, pointing inward the object.

Any contact force $\mathbf{f}_i$ at the contact point $\mathbf{p}_i$ can hence be expressed as in Eq. (5). Sum of the non-negative coefficients $\alpha_{i,j}$ describes the amplitude of the normal component of the contact force $\mathbf{f}_i$ as in Eq. (6). The contact wrench $\mathbf{w}_i$ produced by the contact force $\mathbf{f}_i$ is written in Eq. (7). The wrench space of the grasp configuration $\mathbf{u}$ is denoted as W shown in Eq. (8).

$$\mathbf{f}_i = \sum_{j=1}^{m} \alpha_{i,j} \mathbf{d}_j(\mathbf{p}_i). \tag{5}$$

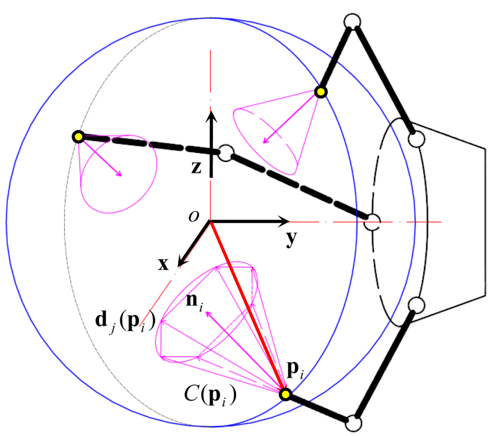

Fig. 2. Frictional point contacts on an object.

$$\mathbf{f}_i \cdot \mathbf{n}_i = \sum_{j=1}^{m} \alpha_{i,j}\mathbf{d}_j(\mathbf{p}_i) \cdot \mathbf{n}_i = \sum_{j=1}^{m} \alpha_{i,j}. \tag{6}$$

$$\mathbf{w}_i = \begin{bmatrix} \mathbf{f}_i \\ \mathbf{p}_i \times \mathbf{f}_i \end{bmatrix} = \sum_{j=1}^{m} \alpha_{i,j}\mathbf{w}_{i,j} \text{ and } \mathbf{w}_{i,j} = \begin{bmatrix} \mathbf{d}_j(\mathbf{p}_i) \\ \mathbf{p}_i \times \mathbf{d}_j(\mathbf{p}_i) \end{bmatrix}. \tag{7}$$

$$W = \text{Convex Hull}\left(\bigcup_{i=1}^{n}\{w_{i,1}, \ldots, w_{i,m}\}\right). \tag{8}$$

The Q distance[29] (including the Q^+ and Q^- distances) that is used for grasp quality quantification is the separation or penetration pseudo-distance between the wrench space W and a $\mathbf{0}$ set (the original of the wrench space). The Q^+ distance quantifies the separation distance as in Eq. (9), following the definition from Eq. (1).

When the separation distance is zero, the Q^- distance shall be calculated as the penetration distance as in Eq. (10), following the definition from Eq. (2):

$$d_Q^+(\mathbf{u}) = d_s(W, \mathbf{0}), \tag{9}$$

$$d_Q^-(\mathbf{u}) = d_p(W, \mathbf{0}), \tag{10}$$

where the grasp configuration $\mathbf{u}$ determines the contact points $\mathbf{p}_i$; the contact points $\mathbf{p}_i$ give the elementary wrench $\mathbf{w}_{i,}$ from Eq. (7).

The pseudo-distance formulation is differentiable.[29,30] The differentiability directly enables this gradient-based reach-to-grasp algorithm.

3. Descriptions of the Synergy-Based Hand and Formulation of the Grasp Planning Algorithm

In Sec. 3.1, the description of the synergy-based hand is presented. Then the formulation of the gradient-based grasp planning algorithm is reported in Sec. 3.2.

3.1. *Synergy-based hand*

There are 11 joints in the synergy-based hand: 3 for the thumb, while 2 for the index, the middle, the ring and the little fingers, respectively. The T, I, M, R, and L letters indicate the thumb, the index, the middle, the ring, and the little fingers, respectively. Abbreviations of *rot*, *mcp*, *ip*, *abd*, *pip*, and *dip* indicate the rotation, the metacarpophalangeal, the interphalangeal, the abduction, the proximal, and the distal interphalangeal joints, respectively. To simplify the hand structure, the T_{ip} joint and the *dip* joints are fixed to 20°. In addition, the T_{mcp} joint is coupled to the T_{abd} joint and the *pip* joints are coupled to the *mcp* joints of the fingers with a ratio of 1: 1 for simplification.

There are 6 degrees of freedom in the synergy-based hand: 2 for the thumb and 1 for each finger. There are 3 phalanges in each finger and the proximal, middle, and distal phalange are indexed as 1, 2, and 3, respectively. The synergy-based hand is shown in Fig. 3, also showing the phalange indices for the little finger.

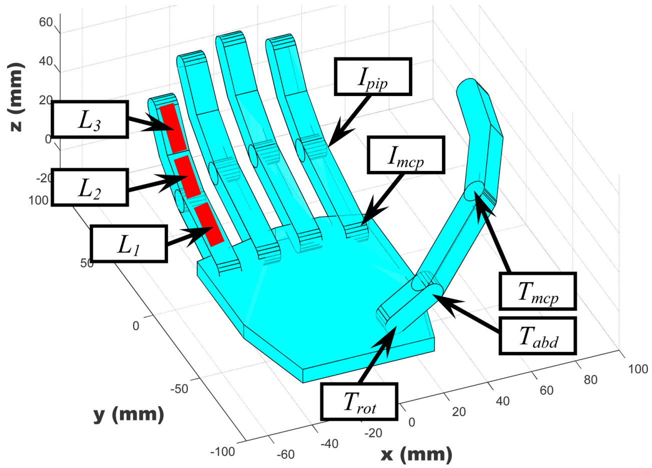

Fig. 3. Structure and joint assignments of the synergy-based hand.

Table 1. Structural parameters of the simulated hand (unit: mm).

	Thumb	Index	Middle	Ring	Little
Distal phalange	27	20	21	21	20
Intermediate phalange	—	25	28	27	21
Proximal phalange	32	47	48	46	40
Metacarpal	46	—	—	—	—

The phalange lengths were first set according to a study on hand anatomy.[33] These original phalange lengths.[33] have the index finger about 10 mm shorter than the middle finger. This difference can negatively impact the stability of the planned grasps, although this may be true for actual human anatomy. Then the phalange lengths were modified according to another study.[34] As shown in Table 1, the phalange lengths are rounded to millimeters.

There are six actuated joints (the T_{rot}, T_{abd}, I_{mcp}, M_{mcp}, R_{mcp}, and L_{mcp} joints) in the synergy-based hand, and the hand pose is represented as a six-dimensional pose vector $\mathbf{\Psi}$, including the six joint angles. The postural synergies of the hand can be extracted from a group of grasping and pinching poses. In the previous study,[35] the anthropomorphic hand grasped a dozen of daily-life objects. Then the extracted postural synergies ($\mathbf{s}_1$ and $\mathbf{s}_2$) and the average pose $\bar{\mathbf{\Psi}}$ are presented in Table 2. A hand pose can be approximated as in Eq. (11):

$$\mathbf{\Psi} = \bar{\mathbf{\Psi}} + [\,\mathbf{s}_1 \quad \mathbf{s}_2\,][\,z_1 \quad z_2\,]^T, \tag{11}$$

where z_1 and z_2 are the synergy variables. Elements of the postural synergies s_1 and s_2 are listed as the matching cells in Table 2.

Table 2. The extracted postural synergies (unit: rad).

	T_{rot}	T_{abd}	I_{mcp}	M_{mcp}	R_{mcp}	L_{mcp}
Synergy1 (s_1)	−0.2137	0.0490	0.0676	0.2573	0.2991	0.3279
Synergy2 (s_2)	−0.1731	−0.1318	−0.3853	−0.4756	−0.4316	−0.3440
$\bar{\mathbf{\Psi}}$	1.2140	0.4030	0.6616	0.7145	0.7723	0.8875

The hand pose will change when the synergy variables of z_1 and z_2 are varied. The hand poses are shown in Fig. 4 while changing z_1 and z_2 between $[-1, 1]$.

3.2. *Gradient-based grasp planning*

The grasp configuration $\mathbf{u}$ is defined as a vector $[p_x p_y p_z \phi_1 \phi_2 \phi_3 z_1 z_2]^T$, which includes the palm's position (p_x, p_y, and p_z), the palm's orientation (three XYZ Euler angles: ϕ_1, ϕ_2, and ϕ_3), and the synergy variables (z_1 and z_2).

Based on the pseudo-distance formulation, this paper proposes a scaled Q distance (the sQ distance) for predicting the grasp quality and the contact pseudo-distance (the cP distance) to quantify the contact condition. In the grasp planning algorithm, the grasp status includes the cP and the sQ distances.

For a precision grasp, the contact condition (namely the cP distance) consists of five pseudo-distances between each fingertip (a single point) and the object

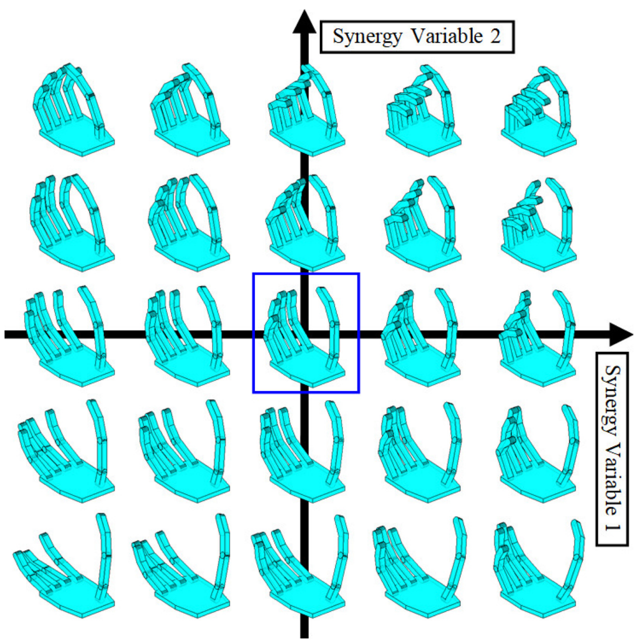

Fig. 4. Hand poses under different synergy variables on the synergy plane with the average pose shown inside the central blue box.

(e.g., a point cloud representation): $\mathbf{g}_{cP\_precision} = [g_{T0}\, g_{I0}\, g_{M0}\, g_{R0}\, g_{L0}]^T$, where the subscripts of T, I, M, R or L stand for the five fingers and 0 indicates the fingertip.

For a power grasp, the contact condition is different and it involves possibly more contact points. In the proposed framework, one point is assumed on each of the three phalanges of each finger, while one more point is assumed on the palm. Then the contact condition for the power grasp consists of 16 pseudo-distances between the object and the points on the hand: $\mathbf{g}_{cP\_power} = [g_{T1}\, g_{T2}\, g_{T3}\, g_{I1}\, g_{I2}\, g_{I3}\, g_{M1}\, g_{M2}\, g_{M3}\, g_{R1}\, g_{R2}\, g_{R3}\, g_{L1}\, g_{L2}\, g_{L3}\, g_P]^T$, where the subscripts of *1*, *2*, *3* stand for the phalange indices, and P stands for the palm.

The presented framework attempts to predict the grasp quality when the hand is relatively far from the object to be grasped. Then in the grasp planning process, the palm's position, orientation, and the hand's postural synergy variables can be continuously adjusted, aiming to reach a stable grasp with minimal trials.

As illustrated in Fig. 5, the to-be-grasped object is at a location away from the hand, touching none of the fingers. Then the object can be proportionally scaled such that the scaled object would get in touch with the points of the hand.

For a precision grasp, the contact points will be on the fingertips. For a power grasp, the contact points will be on the phalanges and the palm.

Using the contact points between the hand and the scaled objects, the sQ distance (g_{sQ}) can be calculated using Eqs. (9) and (10), where the contact wrench $\mathbf{w}_i$ is produced from the contact points and the surface normal unit vectors of the scaled object.

Then a grasp status vector $\mathbf{g}(\boldsymbol{g}_{precision}$ or $\boldsymbol{g}_{power})$ for the reach-to-grasp task can be defined as in Eqs. (12) and (13) for precision grasp and power grasp, respectively.

$$\mathbf{g}_{precision} = \left[\, \mathbf{g}^{\,T}_{cP\_precision} \quad g_{sQ} \,\right]^T \in \Re^{6\times 1}. \tag{12}$$

$$\mathbf{g}_{power} = \left[\, \mathbf{g}^{\,T}_{cP\_power} \quad g_{sQ} \,\right]^T \in \Re^{17\times 1}. \tag{13}$$

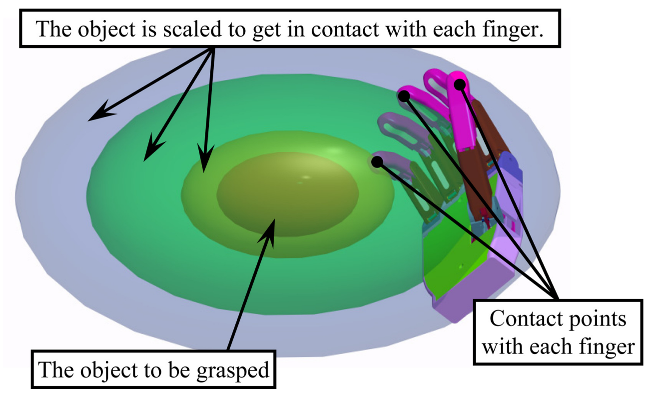

Fig. 5. The scaled to-be-grasped object leading to the sQ distance.

According to the definition of the Q and sQ distances, a negative value indicates a stable grasp. The smaller the value is, the bigger stability margin the grasp has. Hence, the grasp status vector $\mathbf{g}$ will always have known target values: enough contact points with a negative g_{sQ} value. The specific $\mathbf{g}_{cP\_precision}$, $\mathbf{g}_{cP\_power}$, and g_{sQ} values are detailed in Sec. 4.

The grasp status vector $\mathbf{g}$ depends on the grasp configuration $\mathbf{u} = [p_x p_y p_z \phi_1 \phi_2 \phi_3 z_1 z_2]^T$. Then using the derivative of the pseudo-distance formulation,[30] the Jacobian matrix $\mathbf{J}_\mathbf{g}$ can be derived as in Eq. (14).

$$\mathbf{J}_\mathbf{g} = \left[\frac{\partial \mathbf{g}}{\partial p_x}\ \frac{\partial \mathbf{g}}{\partial p_y}\ \frac{\partial \mathbf{g}}{\partial p_z}\ \frac{\partial \mathbf{g}}{\partial \phi_1}\ \frac{\partial \mathbf{g}}{\partial \phi_2}\ \frac{\partial \mathbf{g}}{\partial \phi_3}\ \frac{\partial \mathbf{g}}{\partial z_1}\ \frac{\partial \mathbf{g}}{\partial z_2}\right]$$
$$= \begin{bmatrix} \frac{\partial g_1}{\partial p_x} & \frac{\partial g_1}{\partial p_y} & \frac{\partial g_1}{\partial p_z} & \frac{\partial g_1}{\partial \phi_1} & \frac{\partial g_1}{\partial \phi_2} & \frac{\partial g_1}{\partial \phi_3} & \frac{\partial g_1}{\partial z_1} & \frac{\partial g_1}{\partial z_2} \\ \vdots & \vdots & \vdots & \vdots & \vdots & \vdots & \vdots & \vdots \\ \frac{\partial g_n}{\partial p_x} & \frac{\partial g_n}{\partial p_y} & \frac{\partial g_n}{\partial p_z} & \frac{\partial g_n}{\partial \phi_1} & \frac{\partial g_n}{\partial \phi_2} & \frac{\partial g_n}{\partial \phi_3} & \frac{\partial g_n}{\partial z_1} & \frac{\partial g_n}{\partial z_2} \end{bmatrix}^T. \tag{14}$$

Then an iterative gradient-based algorithm for planning the reach-to-grasp tasks can be constructed as in Fig 6. This algorithm is inspired by the resolved rates algorithm for Jacobian-based manipulator control.[36]

Starting with the intended target grasp status vector $\mathbf{g}^t$ and the current grasp status vector $\mathbf{g}^c$, the difference between the value of the two vectors can be obtained

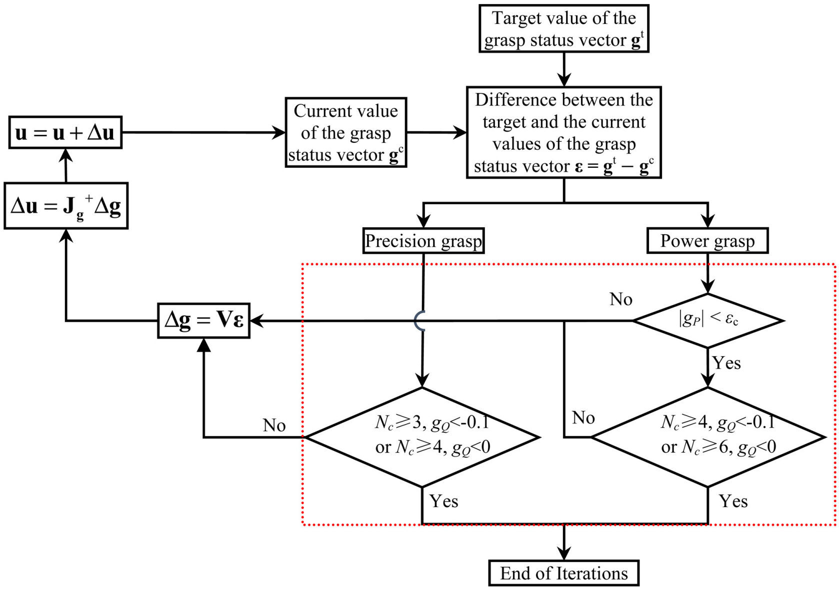

Fig. 6. Flow chart of the gradient-based grasp planning algorithm.

as $\boldsymbol{\varepsilon} = \mathbf{g}^t – \mathbf{g}^c$. If the stop criterions are satisfied, the algorithm will be terminated and a stable grasp is achieved.

The stop criterions are presented in the red dashed box in Fig. 6.

N_c represents the number of contact points. Since the fingers are not independently driven, it is highly possible that not all the fingers touch the object surface at the same time. A point is considered in contact if the corresponding element in the $\mathbf{g}_{cP\_precision}$ or $\mathbf{g}_{cP\_power}$ vectors is smaller than a threshold ε_c.

While the sQ distance attempts to predict the grasp stability, the actual grasp stability is indicated by the Q distance whose calculation shall exclude the non-contacting points on the hand. Hence, the Q distance (g_Q) should be used in the stop criterion for grasp planning. In other words, g_{sQ} is calculated via the contact points of the virtually scaled object with the hand and it is used in the iterative process for hand posture adjustments. The g_Q value is calculated from the actual contact points of the object. A Q distance value of -0.1 is typical from the previous investigation.[29]

If a precision grasp is planned, when N_c is larger or equal to 3, the g_Q value shall be smaller than -0.1; when N_c is larger or equal to 4, the g_Q value shall be negative. If a power grasp is planned, the $|g_P|$ value should be first smaller than the threshold ε_c, indicating a contact point on the palm. Otherwise, it will not be considered a power grasp. Then when N_c is larger or equal to 4, the g_Q value shall be smaller than -0.1; when N_c is larger or equal to 6, the g_Q value shall be negative.

If the stop criterions are not satisfied, the desired increment of the grasp status vector $\Delta\mathbf{g}$ is obtained as in Eq. (15). The incremental change of the grasp configuration $\Delta\mathbf{u}$ is obtained as in Eq. (16), where the Jacobian $\mathbf{J_g}$ is from Eq. (14). The singularity robust formulation is used. Then the grasp configuration $\mathbf{u}$ is updated as $\mathbf{u} = \mathbf{u} + \Delta\mathbf{u}$. Using the updated grasp configuration $\mathbf{u}$, the new grasp status vector $\mathbf{g}$ can be obtained. This would start a new iteration:

$$\Delta\mathbf{g} = \mathbf{V}\boldsymbol{\varepsilon}, \tag{15}$$

where $\mathbf{V}$ is a diagonal control matrix for adjusting the iteration step lengths.

$$\Delta\mathbf{u} = \mathbf{W}^{-1}\mathbf{J}_{\mathbf{g}}^{T}(\mathbf{J_g}\mathbf{W}^{-1}\mathbf{J}_{\mathbf{g}}^{-1} + \lambda\mathbf{I})^{-1}\Delta\mathbf{g}, \tag{16}$$

where $\mathbf{W}$ is a weight matrix for adjusting the normalization of the position and orientation elements of the grasp configuration vector $\mathbf{u}$; λ is set at 10^{-5}, depending on whether the smallest Eigenvalue of $\mathbf{J_g}\mathbf{W}^{-1}\mathbf{J}_{\mathbf{g}}^{-1}$ is smaller than 10^{-5}.

4. Computational Experiments

In order to demonstrate the effectiveness of the proposed algorithm, a series of computational experiments were carried out. The reach-to-grasp tasks including precision and power grasp for several objects are planned, as presented in Secs. 4.1 and 4.2, respectively. The friction coefficient between the object and the fingers is set at 0.3. The friction cone is linearized by an eight-sided polyhedral cone ($m = 8$).

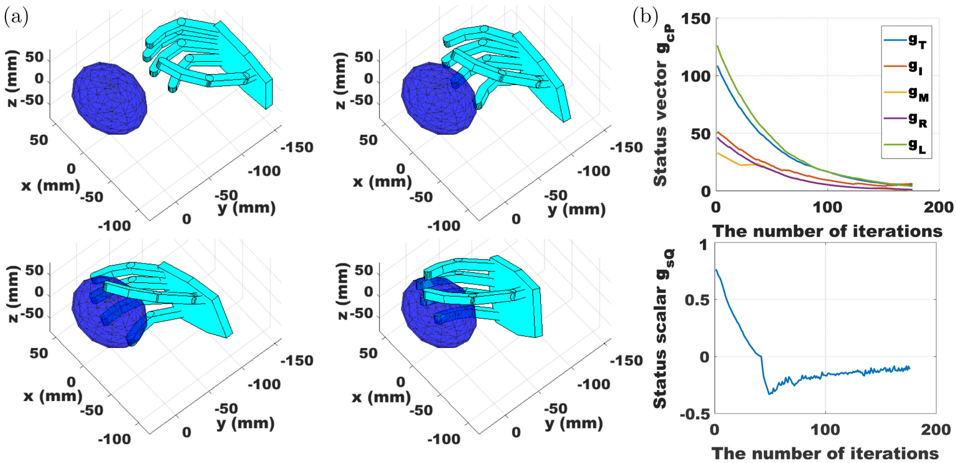

Fig. 7. Reach to grasp an ellipsoid: (a) hand poses and (b) status vector $\mathbf{g}_{\text{precision}}$.

4.1. *Precision grasps*

The proposed gradient-based iterative grasp planning algorithm was first tested for the precision grasp of an ellipsoid as shown in Fig. 7.

The fingertip points can be calculated from the grasp configuration $\mathbf{u}$ that includes the hand's position, orientation, and the synergy variables. For an ellipsoid with three axes of 30 mm, 40 mm and 50 mm whose center is located at the origin of the reference frame, the cP distances of the five fingers (g_{T0}, g_{I0}, g_{M0}, g_{R0}, and g_{L0}) were calculated according to the definitions of the pseudo-distance. Using the positions of the fingertips while the hand approaches the ellipsoid, the sQ distance (the g_{sQ} value) can be calculated from Eqs. (9) and (10).

In the implemented algorithm, the target grasp status vector $\mathbf{g}^t$ is set as $[0 \cdots 0 {-1}]^T$, aiming at a scenario where the fingers fully touch the object with a sufficient stability margin. The control matrix $\mathbf{V} = \text{diag}\,(10^{-3}, \ldots, 10^{-3}) \in \mathcal{R}^{6\times6}$ adjusts the iteration step lengths. The contact threshold ε_c is set at 5, considering the thickness of the fingers and palm.

The hand poses and the values of the grasp status vector $\mathbf{g}_{precision}$ for the reach-to-grasp motion of the ellipsoid are shown in Fig. 7 as well as in the multimedia extension.

At the beginning of the reach-to-grasp process, the hand in its average pose is placed away from the ellipsoid to be grasped. The sQ distance (the g_{sQ} value) is 0.7647, predicting an unstable grasp. Under this proposed algorithm, the hand first opens its fingers while approaching the ellipsoid and then closes its fingers to achieve a stable grasp. The iterations stopped after the 176th step and the total simulation time in MATLAB 2015 was 54 s on a laptop with an Intel i5-2430M CPU and 4 GB memory. The terminating cP distances of the five fingers (g_{T0}, g_{I0}, g_{M0}, g_{R0}, and g_{L0})

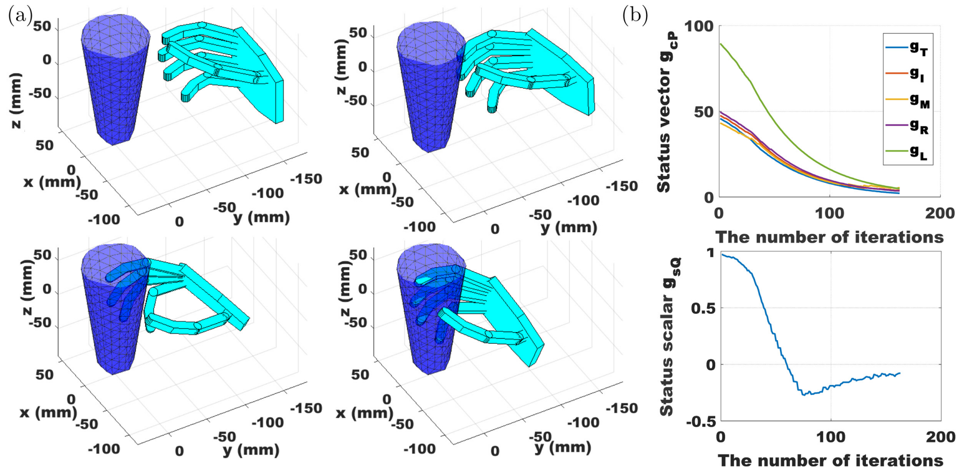

Fig. 8. Reach to grasp a cup: (a) hand poses and (b) status vector $\mathbf{g}_{\text{precision}}$.

are 4.9722, 6.0495, 0.6209, 1.1141, and 4.0755, respectively, with the sQ distance of -0.1123. The Q distance is -0.0792. And the stop criterion was satisfied.

Additional computational experiments including grasping a cup, a bell and a goblet are presented in Figs. 8–10, respectively, and in the multimedia extension.

When the precision grasp planning of a cup was terminated after 163 iterations, the cP distances of the five fingers (g_{T0}, g_{I0}, g_{M0}, g_{R0}, and g_{L0}) are 2.1721, 3.8856, 5.3117, 3.5313, and 4.9242, respectively, with the sQ distance of -0.0798 and the Q distance of -0.0570. The total simulation time on the same laptop is 60 s.

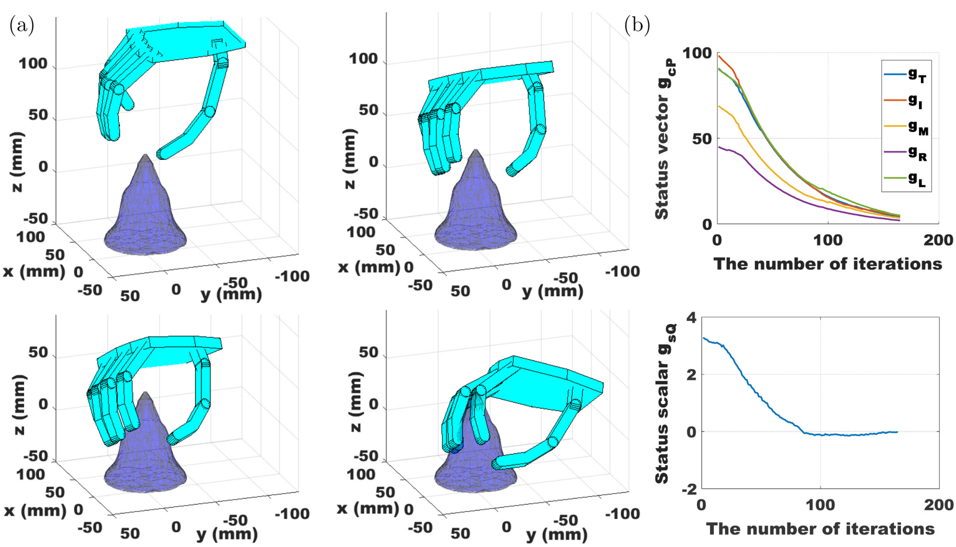

Fig. 9. Reach to grasp a bell: (a) hand poses and (b) status vector $\mathbf{g}_{\text{precision}}$.

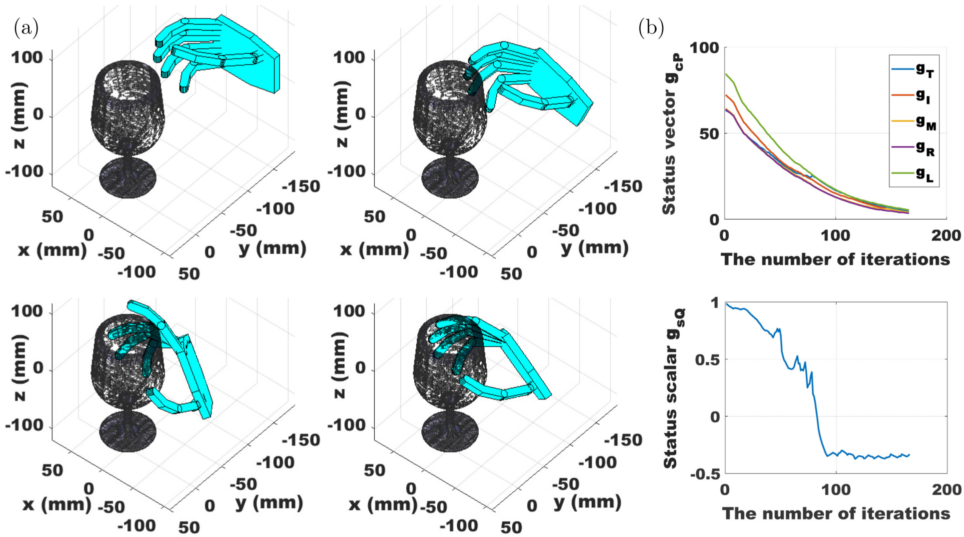

Fig. 10. Reach to grasp a goblet: (a) hand poses and (b) status vector $\mathbf{g}_{\text{precision}}$.

When the precision grasp planning of a bell was terminated after 165 iterations, the cP distances of the five fingers (g_{T0}, g_{I0}, g_{M0}, g_{R0}, and g_{L0}) are 4.1064, 4.6548, 3.4908, 2.0295, and 4.8831, respectively, with the sQ distance of -0.0260 and the Q distance of -0.0260. When the precision grasp planning of a goblet was terminated after 166 iterations, the cP distances of the five fingers (g_{T0}, g_{I0}, g_{M0}, g_{R0}, and g_{L0}) are 4.9334, 3.9520, 3.9784, 3.4377, and 5.3372, respectively, with the sQ distance at -0.3315 and the Q distance at -0.1513.

The computational time is a bit long. The main reason is that each of the linear programming problems implemented in MATLAB takes 30–50 ms. Then each iteration takes 0.3 to 0.4 s. Varying the iteration steps controlled by the matrix $\mathbf{V}$ may further reduce the total iteration time.

4.2. *Power grasps*

Then the proposed algorithm was also tested for planning power grasps of several objects. The hand poses and the values of the grasp status vector $\mathbf{g}_{power}$ for the power grasp of an ellipsoid are shown in Fig. 11 and in the multimedia extension. The other computational experiments including power grasping the cup, the bell, and the goblet are presented in Figs. 12–14, respectively, and in the multimedia extension.

While planning a power grasp, the target grasp status vector $\mathbf{g}^t$ and the contact threshold ε_c are the same as the values in Sec. 4.1. The control matrix $\mathbf{V} = \text{diag}(10^{-3}, \ldots, 10^{-3}) \in \mathcal{R}^{17\times 17}$ is used because the power grasp involves more contact points.

When the power grasp planning of an ellipsoid was terminated after 63 iterations, the sQ distance is -0.2209 and the Q distance is -0.0625. The total simulation time

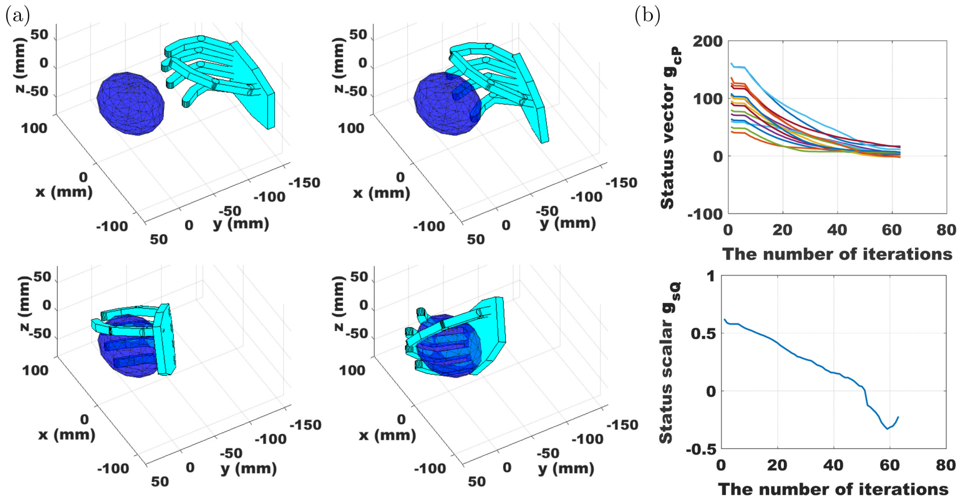

Fig. 11. Reach to grasp an ellipsoid: (a) hand poses and (b) status vector $\mathbf{g}_{\mathrm{power}}$.

on the same laptop is 59 s. There are 10 contact points with the ellipsoid, including nine on the finger phalanges and one on the palm. Now each iteration takes more time because more points are involved.

When the power grasp planning of a cup was terminated after 69 iterations, the sQ distance is -0.4377 and the Q distance is -0.1017. The total simulation time is 80 s.

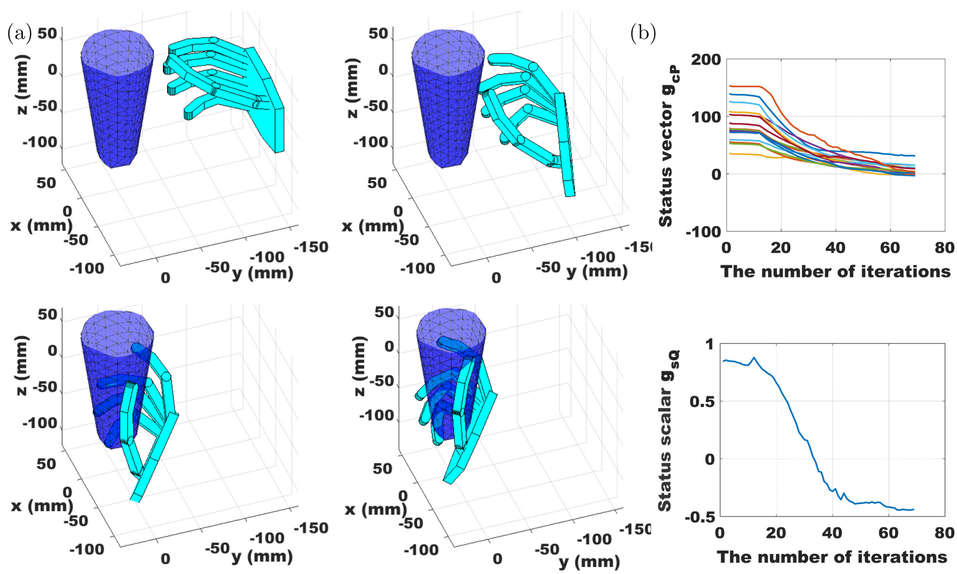

Fig. 12. Reach to grasp a cup: (a) hand poses and (b) status vector $\mathbf{g}_{\mathrm{power}}$.

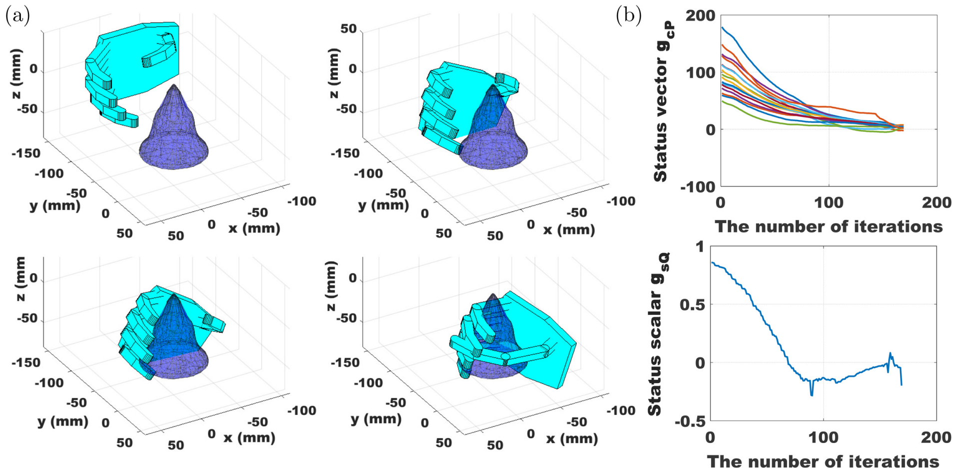

Fig. 13. Reach to grasp a bell: (a) hand poses and (b) status vector $\mathbf{g}_{\text{power}}$.

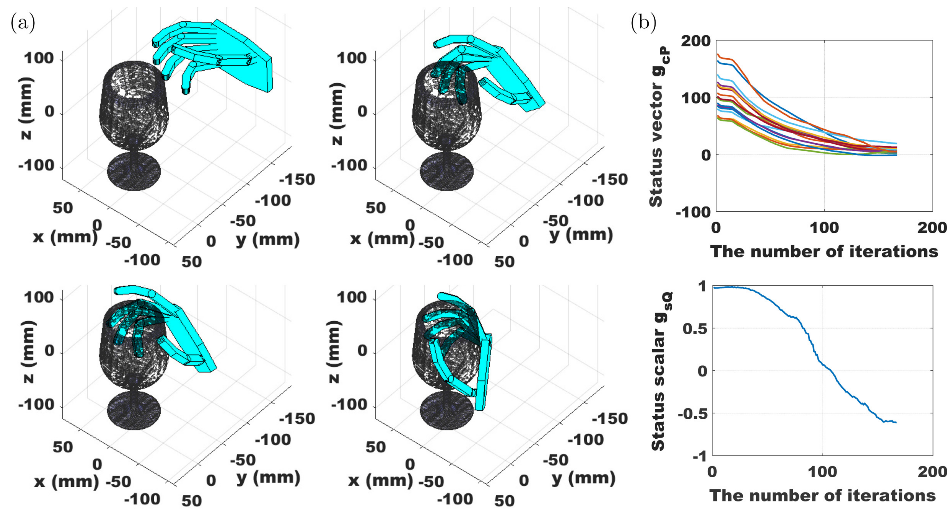

Fig. 14. Reach to grasp a goblet: (a) hand poses and (b) status vector $\mathbf{g}_{\text{power}}$.

When the power grasp planning of a bell was terminated after 169 iterations, the sQ distance is -0.1979 and the Q distance is -0.1386. As for the power grasp of a goblet in Fig. 14, the sQ distance ends at -0.6010 and the Q distance is -0.2574.

5. Conclusion

This paper proposes a gradient-based iterative algorithm for reach-to-grasp planning on a synergy hand, through grasp quality prediction, aiming at adjusting the position, the orientation, and the postural synergies of a hand when the hand approaches the object to be grasped, aiming to achieve stable grasps with minimal attempts. The grasp quality measurement and the contact condition of the fingers are adopted from a highly efficient pseudo-distance formulation.

Multi-fingered precision or power grasps can be intentionally planned conveniently under the same framework, via specifying different contact conditions. Several numerical simulation case studies are presented to demonstrate the effectiveness of the proposed algorithm. However, only the geometry information is used for the planning, the computer tries to find the optimum result of the object function, which will lead the grasp process is not like the human habits and the trajectory of grasp planning is still a bit vibration especially the rotations of palm. To solve these problems, more attention should be paid in the planning process.

Variable iteration step lengths will be investigated to further improve the computational efficiency in the near future. Coupled with point cloud acquisition approaches of an object, the presented planning framework for reach-to-grasp tasks could be one step closer to achieve autonomous grasping.

Acknowledgments

This work was supported by the National Natural Science Foundation of China (Grant Nos. 51722507, 51435010 and 91648103).

References

1. N. Bernstein, The problem of the interrelation of coordination and localization, *Arch. Biol. Sci.* **38** (1935) 1–34.
2. M. Santello, M. Flanders and J. F. Soechting, Postural hand synergies for tool use, *J. Neurosci. Res.* **18** (1998) 10105–10115.
3. M. T. Ciocarlie and P. K. Allen, Hand posture subspaces for dexterous robotic grasping, *The International Journal of Robotics Research* **28** (2009) 851–867.
4. C. Y. Brown and H. H. Asada, Inter-finger coordination and postural synergies in robot hands via mechanical implementation of principal components analysis, in *IEEE/RSJ Int. Conf. on Intelligent Robots and Systems (IROS)* (San Diego, CA, USA, 2007), pp. 2877–2882.
5. K. Xu, H. Liu, Y. Du and X. Zhu, Design of an underactuated anthropomorphic hand with mechanically implemented postural synergies, *Adv. Robotics* **28** (2014) 1459–1474.
6. W. Chen, C. Xiong and S. Yue, Mechanical implementation of kinematic synergy for continual grasping generation of anthropomorphic hand, *IEEE/ASME Trans. Mechatron.* **20** (2015) 1249–1263.
7. C.-H. Xiong, W.-R. Chen, B.-Y. Sun, M.-J. Liu, S.-G. Yue and W.-B. Chen, Design and implementation of an anthropomorphic hand for replicating human grasping functions, *IEEE Trans. Robot.* **32** (2016) 652–671.
8. K. Xu, Z. Liu, B. Zhao, H. Liu and X. Zhu, Composed continuum mechanism for compliant mechanical postural synergy: An anthropomorphic hand design example, *Mech. Mach. Theory* **132** (2019) 108–122.
9. G. C. Matrone, C. Cipriani, E. L. Secco, M. C. Carrozza and G. Magenes, Bio-inspired controller for a dexterous prosthetic hand based on principal components analysis, in

Annual Int. Conf. of the IEEE Engineering in Medicine and Biology Society (EMBS) (Minneapolis, Minnesota, USA, 2009), pp. 5022–5025.
10. F. Ficuciello, G. Palli, C. Melchiorri and B. Siciliano, Experimental evaluation of postural synergies during reach to grasp with the UB Hand IV, in *IEEE/RSJ Int. Conf. on Intelligent Robots and Systems (IROS)* (San Francisco, CA, USA, 2011), pp. 1775–1780.
11. G. Palli, C. Melchiorri, G. Vassura, U. Scarcia, L. Moriello, G. Berselli, A. Cavallo, G. D. Maria, C. Natale, S. Pirozzi, C. May, F. Ficuciello and B. Siciliano, The DEXMART hand: Mechatronic design and experimental evaluation of synergy-based control for human-like grasping, *Int. J. Robot. Res.* **33** (2014) 799–824.
12. J. L. Segil and R. F. F. Weir, Design and validation of a morphing myoelectric hand posture controller based on principal component analysis of human grasping, *IEEE Trans. Neural Syst. Rehabil. Eng.* **22** (2014) 249–257.
13. M. T. Ciocarlie and P. K. Allen, Hand posture subspaces for dexterous robotic grasping, *Int. J. Robot. Res.* **28** (2009) 851–867.
14. M. Gabiccini, E. Farnioli and A. Bicchi, Grasp analysis tools for synergistic underactuated robotic hands, *Int. J. Robot. Res.* **32** (2013) 1553–1576.
15. C. I. Mavrogiannis, C. P. Bechlioulis, M. V. Liarokapis and K. J. Kyriakopoulos, Task-specific grasp selection for underactuated hands, in *IEEE Int. Conf. on Robotics and Automation (ICRA)* (IEEE, Hong Kong, China, 2014), pp. 3676–3681.
16. A. Provenzale, F. Cordella, L. Zollo, A. Davalli, R. Sacchetti and E. Guglielmelli, A grasp synthesis algorithm based on postural synergies for an anthropomorphic arm-hand robotic system, in *IEEE/RAS-EMBS Int. Conf. on Biomedical Robotics and Biomechatronics (BIOROB)* (São Paulo, Brazil, 2014), pp. 958–963.
17. A. Bicchi, M. Gabiccini and M. Santello, Modelling natural and artificial hands with synergies, *Philos. Trans. Roy. Soc. B Biol. Sci.* **366** (2011) 3153–3161.
18. S. Li, X. Sheng and X. Zhu, Modelling and analyzing of postural synergy based underactuated robotic hand with contact and friction constraints, in *IEEE Int. Conf. on Advanced Intelligent Mechatronics (AIM)* (IEEE, Busan, South Korea, 2015), pp. 1229–1234.
19. C. Rosales, R. Suárez, M. Gabiccini and A. Bicchi, On the synthesis of feasible and prehensile robotic grasps, in *IEEE Int. Conf. on Robotics and Automation (ICRA)* (IEEE, Saint Paul, Minnesota, USA, 2012), pp. 550–556.
20. D. Guo, F. Sun, J. Zhang and H. Liu, A grasp synthesis and grasp synergy analysis for anthropomorphic hand, in *IEEE Int. Conf. on Robotics and Biomimetics (ROBIO)* (IEEE, Shenzhen, China, 2013), pp. 1617–1622.
21. G. Averta, F. Angelini, M. Bonilla, M. Bianchi and A. Bicchi, Incrementality and hierarchies in the enrollment of multiple synergies for grasp planning, *IEEE Robot. Autom. Lett.* **3** (2018) 2686–2693.
22. G. C. Matrone, C. Cipriani, E. L. Secco, G. Magenes and M. C. Carrozza, Principal components analysis based control of a multi-DOF underactuated prosthetic hand, *J. Neuroeng. Rehabil.* **7** (2010) 16–28.
23. J. M. Vilaplana and J. L. Coronado, A neural network model for coordination of hand gesture during reach to grasp, *Neural Netw.* **19** (2006) 12–30.
24. T. Geng, M. Lee and M. Hülse, Transferring human grasping synergies to a robot, *Mechatronics* **21** (2011) 272–284.
25. F. Ficuciello, D. Zaccara and B. Siciliano, Learning grasps in a synergy-based framework, in *Int. Symp on Experimental Robotics (ISER)* (Tokyo, Japan, 2016), pp. 125–135.
26. J. Starke, C. Eichmann, S. Ottenhaus and T. Asfour, Human-inspired representation of object-specific grasps for anthropomorphic hands, *Int. J. Hum. Robot.* **17** (2020) 2050008.

27. R. Chattaraj, S. Khan, A. Kumar, B. Bepari and S. Bhaumik, Anthropomorphic grasp generation through probabilistic modelling in an optimised eigen-space, *Electron. Lett.* **53** (2017) 582–584.
28. Z. Liu, Z. Wu, T. Dong, X. Zhu and K. Xu, Reach-to-grasp planning for a synergy-controlled robotic hand based on grasp quality prediction, in *IEEE Int. Conf. on Robotics and Biomimetics (ROBIO)* (Kuala Lumpur, Malaysia, 2018), pp. 778–783.
29. X. Zhu and J. Wang, Synthesis of force-closure grasps on 3-D objects based on the Q distance, *IEEE Trans. Robot. Autom.* **19** (2003) 669–679.
30. X. Zhu, H. Ding and S. K. Tso, A pseudodistance function and its applications, *IEEE Trans. Robot. Autom.* **20** (2004) 344–352.
31. Y. Zheng and K. Yamane, Generalized distance between compact convex sets: Algorithms and applications, *IEEE Trans. Robot.* **31** (2015) 988–1003.
32. R. M. Murray, Z. Li and S. S. Sastry, *A Mathematical Introduction to Robotic Manipulation* (CRC Press, 1994).
33. B. Alexander and K. Viktor, Proportions of hand segments, *Int. J. Morphol.* **28** (2010) 755–758.
34. R. Hamilton and R. A. Dunsmuir, Radiographic assessment of the relative lengths of the bones of the fingers of the human hand, *J. Hand. Surg. Br.* **27** (2002) 546–548.
35. K. Xu, H. Liu, Y. Du, X. Sheng and X. Zhu, Mechanical implementation of postural synergies using a simple continuum mechanism, in *IEEE Int. Conf. on Robotics and Automation (ICRA)* (Hong Kong, China, 2014), pp. 1348–1353.
36. D. E. Whitney, Resolved motion rate control of manipulators and human prostheses, *IEEE Trans. Man-Machine Syst.* **10** (1969) 47–53.

Zenghui Liu received a B.S. degree from the School of Mechanical Engineering, Zhejiang University, Hangzhou, China, in 2014. He is currently pursuing his Ph.D. degree at the University of Michigan–Shanghai Jiao Tong University Joint Institute, Shanghai Jiao Tong University, Shanghai, China. His research interests include prosthetic hands biomechatronics and grasping planning.

Yuyang Chen received a B.S. degree from the School of Mechanical Engineering, Zhejiang University, Hangzhou, China, in 2015. He is currently pursuing his Ph.D. degree in the University of Michigan–Shanghai Jiao Tong University Joint Institute, Shanghai Jiao Tong University, Shanghai, China. His research interests include surgical robots and continuum mechanisms.

Xiangyang Zhu received a B.S. degree from the Department of Automatic Control Engineering, Nanjing Institute of Technology, Nanjing, China, in 1985, the M.Phil. degree in instrumentation engineering and the Ph.D. degree in automatic control engineering, both from Southeast University, Nanjing, China, in 1989 and 1992, respectively. From 1993 to 1994, he was a Postdoctoral Research Fellow with Huazhong University of Science and Technology, Wuhan, China. He joined the Department of Mechanical Engineering as an Associate Professor, Southeast University, in 1995. Since June 2002, he has been with the School of Mechanical Engineering, Shanghai Jiao Tong University, Shanghai, China, where he is currently a Changjiang Chair Professor and the Director of the Robotics Institute. His current research interests include robotic manipulation planning, human–machine interfacing, and biomechatronics. Dr. Zhu received the National Science Fund for Distinguished Young Scholars in 2005.

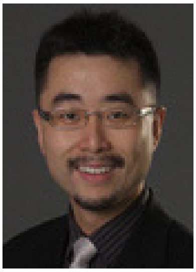

Kai Xu received a B.E. and an M.S. from the Department of Precision Instruments and Mechanology, Tsinghua University, Beijing, China, in 2001 and 2004, respectively, and a Ph.D. (with distinction) from the Department of Mechanical Engineering, Columbia University, New York, NY, in 2009. He is now a Full Professor with the School of Mechanical Engineering, Shanghai Jiao Tong University, Shanghai, China, and the Director of the Robotics Innovation and Intervention Laboratory. His research interests include surgical robots, prosthetic hands, flexible manipulators, special industrial robots, and continuum mechanisms. Prof. Xu has served as a National Expert in China for IEC/ISO JWG9 on medical robotic equipment and systems since 2012 and is currently an Associate Editor for IEEE T-RO. He was selected into the NCET Program by the Ministry of Education, China, in 2010, the Pujiang Scholar Program and the Rising Star Program by the Shanghai metropolitan government in 2011 and 2013, respectively, and received the National Science Fund for Excellent Young Scholars in 2017.